Multiscale computational study of electronic structure and properties of electrochemical nano-systems of perovskites for photovoltaic application

Gusarov, Sergey; Sapelnikova, Karina; Kobryn, Olexander; Shankar, Karthik

National Research Council Canada   Conseil national de recherches Canada

Canada

Multiscale Computational Study of Electronic Structure and Properties of Electrochemical Nano-Systems of Perovskites for Photovoltaic Application

S. Gusarov[a], K. Sapelnikova[b], A. E. Kobryn[a], and K. Shankar[a,c]

[a] National Institute for Nanotechnology,
National Research Council Canada,
11421 Saskatchewan Drive, Edmonton, Alberta, T6G 2M9, Canada
[b] Department of Mechanical Engineering, University of Alberta,
Edmonton, Alberta, T6G 2G8, Canada
[c] Department of Electrical and Computer Engineering, University of Alberta, Edmonton,
Alberta, T6G 2V4, Canada

We present the results of multiscale modelling of electronic and structural properties of organo-halide perovskites of the type $CH_3NH_3PbX_3$ in blends of poly(3-hexylthiophene) (P3HT) or carboxylated poly(3-butylthiophene) (P3BT). For this, we use the Density Functional Theory (DFT) with the Universal Force Field (UFF), and then continue with the Molecular Dynamic simulation (MD). With the former, we optimize the geometry and charge distribution in P3BT and P3HT molecules, analyze electronic orbitals and calculate the absorption spectra. With the latter, we determine structural properties of blends. In addition, the analysis of MD trajectories allows us to better choose the initial positions of P3BT or P3HT molecules in the follow-up DFT analysis which is focused on the study of electronic properties on the border of the perovskite-polymer system. These properties define charge transfer processes from donor to acceptor and are utilized in development of new generation organic solar cells.

Introduction

In recent decades we witness the emergence of a set of new organic thin film electronic devices, including organic photovoltaic cells, organic light-emitting diodes, and organic field-effect transistors [1]. Although the active layers of these devices are composed of amorphous or semi-crystalline organic or polymer films, their basic structure and function have many analogies with inorganic devices. As their application becomes straightforward and inexpensive, the stability, functionality, and efficiency of these devices need improvement. Such a process stimulates the progress of high-mobility organic semiconductors and enriches our knowledge of their electronic structure and transport properties. Inorganic materials, typically characterized by covalent and ionic interactions, offer the potential for high electrical mobility, a wide range of band gaps, a range of dielectric properties, and substantial mechanical and thermal resistance. Organic molecules, which generally interact through hydrogen bonding and van der Waals interactions, provide the possibility of structural diversity, a large degree of polarizability, and mechanical plasticity. Generally, organic-inorganic hybrid research focuses on employing the range of interactions found within organic and inorganic chemistry to

create a composite with some enhanced property relative to that achievable with either organic or inorganic materials alone, or to combine useful properties of the two components within a single material [2]. In some cases, the goal is to search for new phenomena that result from the interaction between the organic and inorganic subunits.

Perovskite structures constitute a wide class of compounds that display an amazing variety of interesting properties. Their family encompasses insulators, piezoelectrics, ferroelectrics, metals, semiconductors, magnetic, and superconducting materials [3]. Their structures are related to these of the mineral perovskites known from the past and can be considered to be derived from a parent phase of general chemical formula ABX_3. Initially dielectric, piezoelectric or ferroelectric behaviors of perovskites today have been expanded into areas which include magnetic ordering, multiferroic properties, electronic conductivity, superconductivity and non-trivial thermal and optical properties [4]. In addition to these purely physical aspects, the perovskite phases also show a wide range of chemical attributes. For example, they are used as electrode materials for solid oxide fuel cells where materials with high oxide ion conductivity, electronic conductivity and mixed ionic-electronic conductivity are required. Finally, many perovskite phases show useful catalytic and redox behavior, often dependent upon the presence of chemical defects in the phase. Both chemical and physical properties of any member of the ABX_3 structural form can be tuned over wide ranges by relatively simple substitution into all or some of the A-, B- and X-sites. This wide-ranging flexibility includes the formation of perovskites in which the A cation is replaced by an organic molecule, typified by the perovskite methylammonium lead chloride, bromide, or iodide, now intensely studied as the next generation photovoltaic cells.

The aim of this study is to provide a compact insight into the modeling and rational design recommendations of perovskite based organic photovoltaic cells. We focus on the organic-inorganic hybrid materials of the type $CH_3NH_3PbX_3$, X = Cl, Br. Typically, the formation of perovskite units from their ionic precursors is studied in solvents with various hydrophobicity, e.g. in water H_2O or pentane C_5H_{12}, which is convenient, in particular, to study the polarity effects. Here we report about the modeling of perovskites in the contact with the blends of carboxylated poly(3-butylthiophene) (P3BT) and poly(3-hexylthiophene) (P3HT), because these materials are sometimes considered as building blocks in the field of organic electronics, including organic solar cells [5,6]. To get an insight into the electronic structure of the systems we use the Density Functional Theory (DFT), while to acquire structural and dynamical properties we run Molecular Dynamics (MD) simulation. The necessity for such a multiscale approach is justified by a number of reasons, including: (i) stochastic nature of motion and interaction of polymeric molecules near the surface; (ii) large size of the perovskite subsystem, because we need many elementary cells together to form a decent surface. Alternatively, structural and thermodynamic properties can be obtained from a version of integral equation theory of molecular liquids which is known as the Reference Interaction Site Model (RISM) or one of its generalizations [6-8]. Multiscale modeling of perovskite systems in melts of P3BT or P3HT with combination of DFT and RISM approaches will be reported elsewhere.

Results and Analysis

On the first stage of our study, we utilize the molecular dynamics simulations (MD) in order to get the most favorite orientations of polymer molecules (P3BT, P3HT) of hoping layer interacting with the perovskite surface. That allow us to avoid the computationally expensive density functional theory (DFT) mapping of different possible relative

orientations of polymer molecules on perovskite surface. Moreover, within the MD approach we can accurately model interactions of polymers on the surface with other molecules of the bulk hoping layer. The selected snapshots of trajectories are presented in the Fig. 1 (a,b). The initial structures of $CH_3NH_3PbCl_3$ and $CH_3NH_3PbBr_3$ were taken from [9]. and the perovskite surface is represented by the slab with *6x6* unit cells in slab plain (*001*) and thickness 12 *A*. The orientations of CH_3NH_3 were reoptimized and partial charges for perovskite s and polymers were calculated by DFT with PBE functional [10] and DND numerical basis set [11] implemented into DMol3 computational chemistry package [12]. The force field parameters are taken from UFF [13]. The using of UFF is explained my missing the parameters for Pb atom in most popular FF fitted to experimental data (like GROMOS or AMBER), from other site there is a number of works showing that UFF could be used for modeling of accurate geometries for adsorption (e.g. see [14]). Next, the molecular dynamics simulations were performed with NVT ensemble (T=298K, density =1.3 g/cm3) (LAMMPS molecular dynamics simulation package [15]). The molecular structure of amorphous polymeric layer can be characterized in terms of the atomic radial distribution functions, gab(r), which, in our case, give the probabilities of finding an atom of type a (polymer molecule) at a distance r away from a center atom b of perovskite surface (Pb or halogen). The resulting radial distribution functions (RDF's) are presented on Figure 2 (*a-f*). They clearly show the trend of polymer molecules to orient to surface atoms by Sulphur sites, with higher preference to *Pb* site. This trend is more pronounced for $CH_3NH_3PbBr_3$ perovskite (Figure 2, *c* and *f*) while for $CH_3NH_3PbCl_3$ there is probability to orient by oxygen O1 site (Figure 2, *a* and *d*). Another oxygen (marked as O2) is not interacting with perovskite directly, the maximums of first solvation shell are missing (Figure 2, *b* and *e*).

Next, we studied the electronic structure of perovskite surfaces cleaved by (001) and (110) planes (Figures 3,4). To explore the dependence from the layer thickness we use slabs of different width (Tables 1,2) formed by *4x4* unit cells in slab plain. The effect of polymer melt was represented by the COSMO solvation model [16] with the corresponding dielectric constant (ε=1.3). Here and throughout the electronic structure was modelled by DFT with PBE functional and DNP numerical basis set.

We use the number of parameters to characterize the dependence of electronic structure from layer width, such as induced partial charges of surface sites (*Pb* and halogens), as well as their electrophilic and nucleophilic Fukui indexes (local softness and hardness), which could be used as quantitative indications for chemical reactivity [17]. There are also a number of works showing that Fukui function/indexes could be used for characterization of charge transfer activity (e.g. [18]). We have found that the largest values correspond to nucleophilic Fukui function (compare to electrophilic counterpart) which support the direction of charge transfer from hopping polymer layer to perovskite surface. The position of cleaving plane also plays an important role (see Table I). The gradual increase of the layer thickness leads to oscillatory changes in electronic structure characteristics of perovskite slab with general trend to decrease HOMO-LUMO gap (as expected) and small increase in polarization of surface layer. The similar trend was observed in the study of electronic properties of graphene sheets (e.g. [19]). Such results could be used to tune the charge transfer properties of perovskite quantum dots interacting with polymer hopping layer. Unfortunately, due to limitation of DFT we cannot model the larger systems which will possibly lead to convergence of all characteristic with the decreasing of the interaction between surface layers. For the (110) slab we also study the effect of removing CH_3NH_3 molecule from surface layer. This

leads to smaller HOMO-LUMO gap and reduced polarization of neighbor atoms (the corresponding values of induced charges are in parenthesis in Table II).

On the final stage of our work we study the effect of interaction with perovskite layer on electronic properties of *P3BT* and *P3HT* polymers (see Figure 5). The corresponding HOMO-LUMO energy levels diagram for separated (area I) and interacting systems (with different position of cleaving plane, II and III, corresponds to Figure 5) are presented on Figure 6. In general, the interaction with perovskite lead to decreasing the HOMO-LUMO gap of polymers which are located close to perovskite surface. In some cases, we observe small "mixing" of HOMO orbital of polymers with one of highest occupied levels of perovskite (see Figure 6, d, area II). According to our calculations the LUMO orbital of polymer is most affected by the interaction, however that should be verified by more advanced technique (like calculation of transition orbitals) because the regular DFT functionals are optimized to represent the occupied orbitals.

Conclusions

The present study shows the effectiveness of the multiscale approach for treatment of such complex system as polymeric hopping layer interacting with perovskite surface. The use of molecular dynamics allows us to avoid the computationally expensive study of adsorption/interaction of polymers with different kind of perovskite surfaces. The most favorite relative orientations of polymers were used as initial configurations for further optimizations by more accurate DFT calculations. The variation of layer thickness (at least within the range of values comparable with size of unit cell) affects the electronic structure properties, such as HOMO-LUMO gap, induced charges and Fukui indexes. We also see the significant impact of interaction with perovskite surface on electronic structure of polymers. In future studies we are planning to extend the modeling of electronic structure by studying transmission spectra's of "two probe" system (polymer + perovskite surface) which could provide the information about orbitals participating in charge transfer.

Acknowledgments

References

1. D. Yan, H. Wang and B. Du, *Introduction to Organic Semiconductor Heterojunctions*, John Wiley & Sons (Asia) Pte. Ltd., Singapore (2010).
2. D. B. Mitzi, Synthesis, Structure, and Properties of Organic-Inorganic Perovskites and Related Materials. In: *Progress in Inorganic Chemistry*, Vol. 48, Edited by K. D. Karlin (Wiley, New York, 1999), pp. 1-123.
3. T. Wolfram and S. Ellialtioglu, *Electronic and Optical Properties of d-Band Perovskites*, Cambridge University Press, Cambridge (2006).
4. R. J. D. Tilley, *Perovskites: Structure-Property Relationships*, Wiley, Chichester (2016).

5. A. R. A. Khajeh, K. Shankar and P. Choi, *ACS Appl. Mater. Interfaces*, **5**, 4617 (2013).

6. A. E. Kobryn, S. Gusarov and K. Shankar, *Polymers*, **8**, 136 (2016).

7. A. Kovalenko, A. E. Kobryn, S. Gusarov, O. Lyubimova, X. Liu, N. Blinov and M. Yoshida, *Soft Matter*, **8**, 1508 (2012).

8. D. Nikolić, K. A. Moffat, V. M. Farrugia, A. E. Kobryn, S. Gusarov, J. H. Wosnick and A. Kovalenko, *Phys. Chem. Chem. Phys.*, **15**, 6128 (2013).

9. K.T. Butler, J.M. Frost and A. Walsh, *Mater. Horiz.*, **2**, 228 (2015)

10. J. P. Perdew, K. Burke and M. Ernzerhof, *Phys. Rev. Lett.*, **77**, 3865 (1996).

11. B. Delley, *J. Chem. Phys.*, **92**, 508 (1990).

12. B. Delley, *J. Chem. Phys.*, **94**, 7245 (1991); DMol3™, V6.1, Accelrys, Inc., 10188 Telesis Court, Suite 100, San Diego, CA 92121.

13. A.K. Rappe, C.J. Casewit, K.S. Colwell, W.A. Goddard III, W.M. Skiff, *J. Am. Chem. Soc.* **114**, 10024 (1992)

14. F. Cao, Y. Sun, L. Wang and H. Sun, *RSC Adv.*, **4**, 27571-27581 (2014)

15. S. Plimpton, *J. Comp. Phys.*, **117**, 1-19 (1995); http://lammps.sandia.gov.

16. A., Klamt; G., Schüürmann, *J. Chem. Soc. Perkin Trans.*, **2**, 799, (1993)

17. W. Yang, R. Parr, *Proc. Nat. Acad. Sci. USA* 82, 6723 (1985)

18. J. Korchowiec, T. Uchimaru, *J. Phys. Chem. A*, 102, 10167 (1998)

19. B. Mandal, S. Sarkar, P. Sarkar, *J Nanopart Res*, **14**, 1317 (2012)
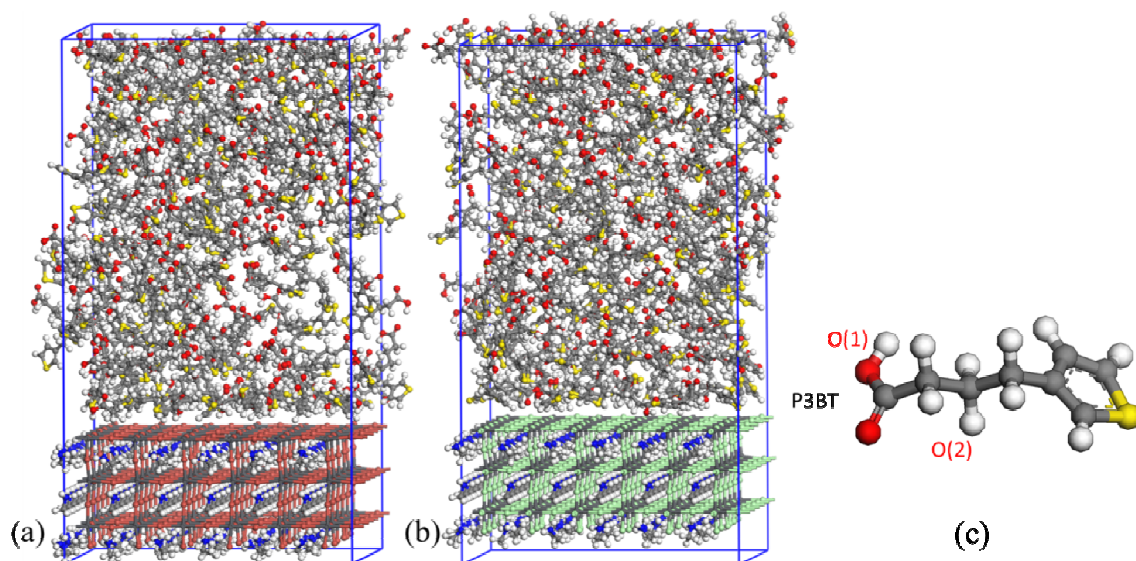
Figure 1, Selected snapshots of molecular dynamics simulation of P2BT polymer melt (density 1.3 g/cm3) on perovskite surface (a - $CH_3NH_3PbBr_3$; b - $CH_3NH_3PbCl_3$)
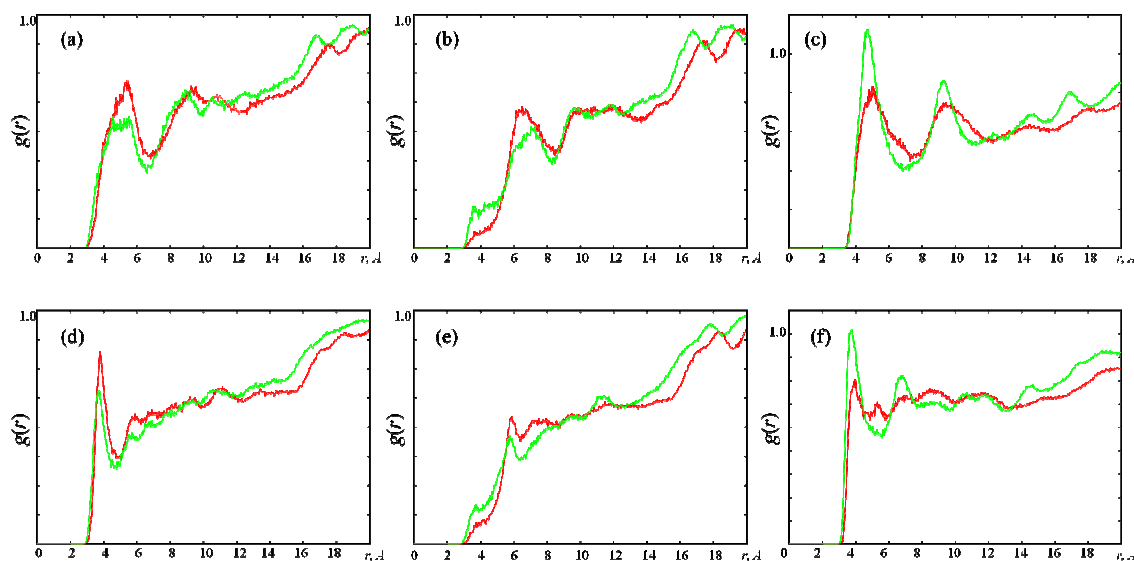

Figure 2, Radial distribution functions between polymer sites (*a* and *d* O(1); *d* and *e* O(2); *c* and *f* - Sulphur;) and atoms (*a,b,c – Pb*; *d,e,f* - halogen) on perovskite surface (red - $CH_3NH_3PbBr_3$; blue - $CH_3NH_3PbCl_3$).

TABLE I. Partial charges and Fukui (f, f^+) indexes of surface atoms at (001) surface layer (L – slab thickness, Δ – HOMO-LUMO gap, W – work function)

	Q	f	f^+
$CH_3NH_3PbBr_3$ L=8.096A, Δ=2.171, W=0.176 (Fig. 3, a)			
Pb	0.560	0.00468	0.0239
Br	-0.395	0.000625	0.00253
Whole Plane	-3.671	0.0950	0.464
$CH_3NH_3PbBr_3$ L=11.896A, Δ=1.397, W=0.18 (Fig. 3, b)			
Pb	0.581	0.000563	0.0203
Br	-0.389	-0.0000938	0.00184

| Whole Plane	-3.159	-0.0120	0.384
$CH_3NH_3PbBr_3$, L=14.868A, Δ=1.498, W=0.163 (Fig. 3, c)			
Pb	0.564	-0.00201	0.0248
Br	-0.391	-0.000438	0.00166
Whole Plane	-3.496	-0.0460	0.450
$CH_3NH_3PbCl_3$, L=8.504A, Δ=2.151, W=0.179 (Fig. 3, d)			
Pb	0.798	0.00403	0.0295
Cl	-0.492	0.00119	0.00178
Whole Plane	-2.964	0.102	0.529
$CH_3NH_3PbCl_3$, L=11.357A, Δ=1.679, W=0.186 (Fig. 3, e)			
Pb	0.810	0.00131	0.0221
Cl	-0.489	-0.000219	0.00238
Whole Plane	-2.695	0.014	0.43
$CH_3NH_3PbCl_3$, L=14.215A, Δ=1.540, W=0.166 (Fig. 3, f)			
Pb	0.811	-0.000125	0.0269
Cl	-0.491	0.000125	0.00166
Whole Plane	-2.801	0.00202	0.483
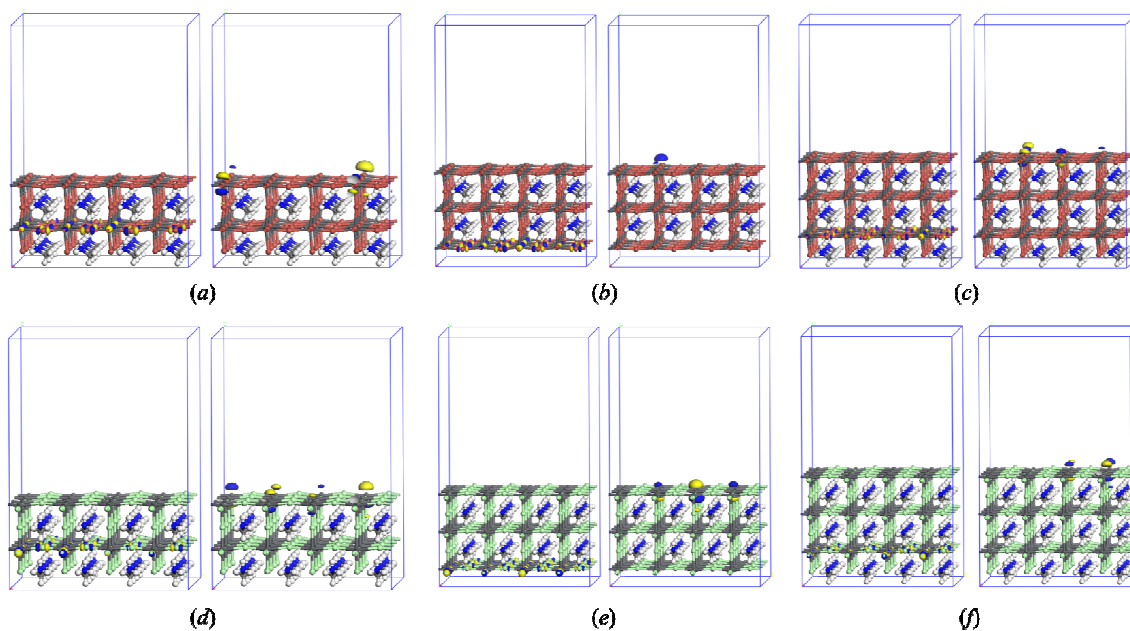
Figure 3, HOMO-LUMO orbitals for the (001) slabs (a,b,c - $CH_3NH_3PbBr_3$; d,e,f - $CH_3NH_3PbBr_3$, see Table I)

TABLE II. Partial charges and Fukui (f, f^+) indexes of halogens atoms at (110) surface layer (L – slab thickness, Δ – HOMO-LUMO gap, W – work function)

	Q	f	f⁺
$CH_3NH_3PbBr_3$, L=7.984A, Δ=0.58, W=0.253 (Fig. 4, a)			
Br	-0.359	-0.000542	0.0133
$CH_3NH_3PbBr_3$, L=12.314A, Δ=0.26, W=0.26 (Fig. 4, b)			
Br	-0.388	-0.0496	0.0513
$CH_3NH_3PbBr_3$, L=12.314A, Δ=0.21, W=0.261 (Fig. 4, d), with defect			
Br	-0.365(-0.259)	-0.0243	-0.0365
$CH_3NH_3PbBr_3$, L=16.653A, Δ=0.63, W=0.267 (Fig. 4, c)			
Br	-0.398	-0.0537	-0.0426

$CH_3NH_3PbCl_3$, L=7.682A, Δ=0.29, W=0.254		
Cl	-0.43575	0.00542	0.00763

$CH_3NH_3PbCl_3$, L=11.667, Δ=1.060, W=0.261		
Cl	-0.463125	-0.016	0.03892

$CH_3NH_3PbCl_3$, L=11.667A, Δ=0.70, W=0.262, with defect		
Cl	-0.447(-0.390)	0.0329	-0.00810

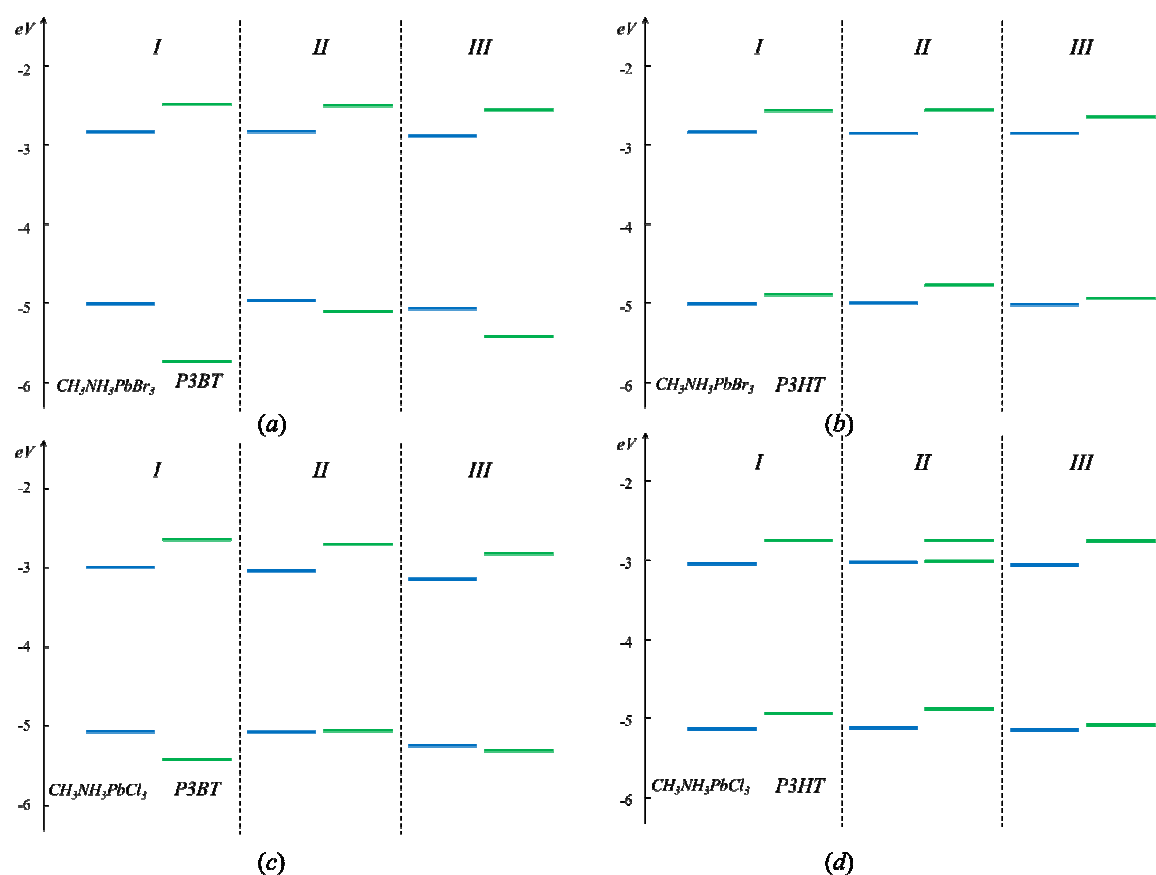| $CH_3NH_3PbCl_3$, L=15.291A, Δ=0.96, W=0.266		
Cl	-0.45425	0.0455	0.0177

(a)　　　(b)

(c)　　　(d)
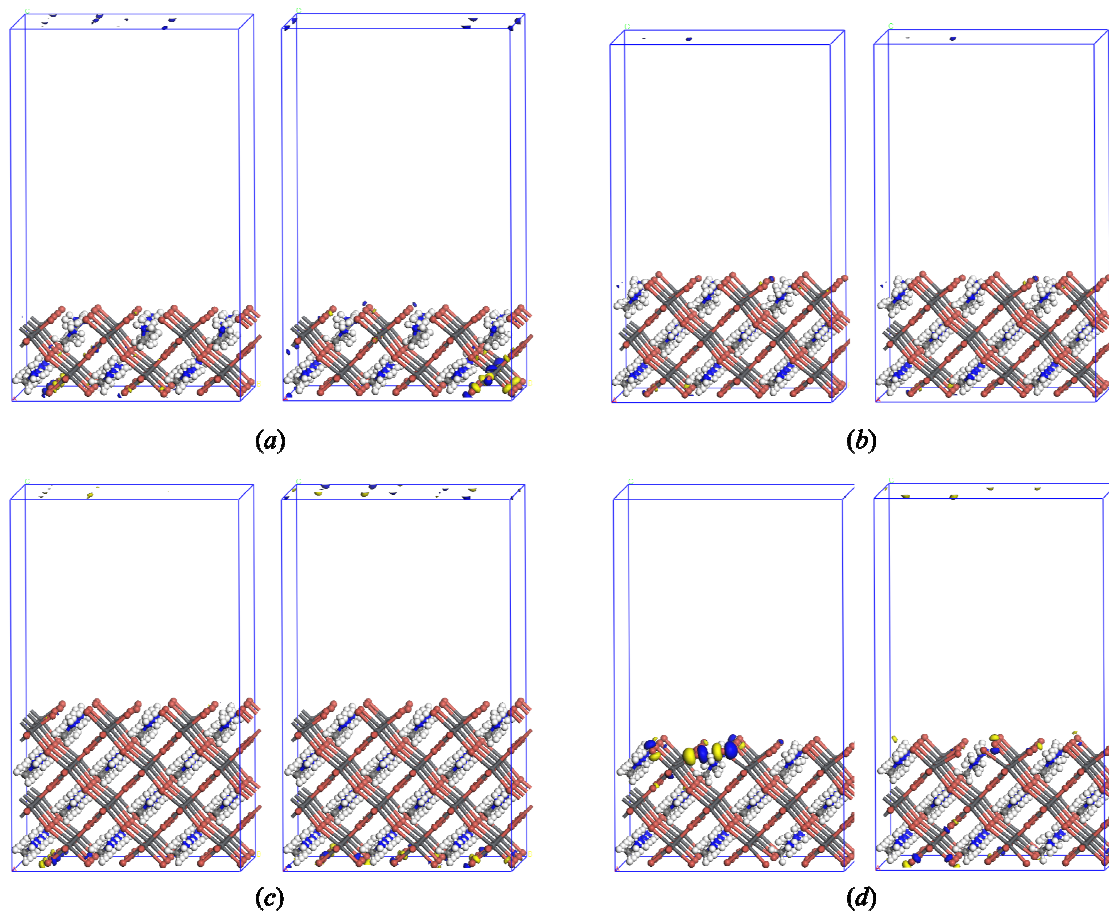
Figure 4, HOMO-LUMO orbitals for the slabs (110) of $CH_3NH_3PbBr_3$ of different thickness (see Table II)
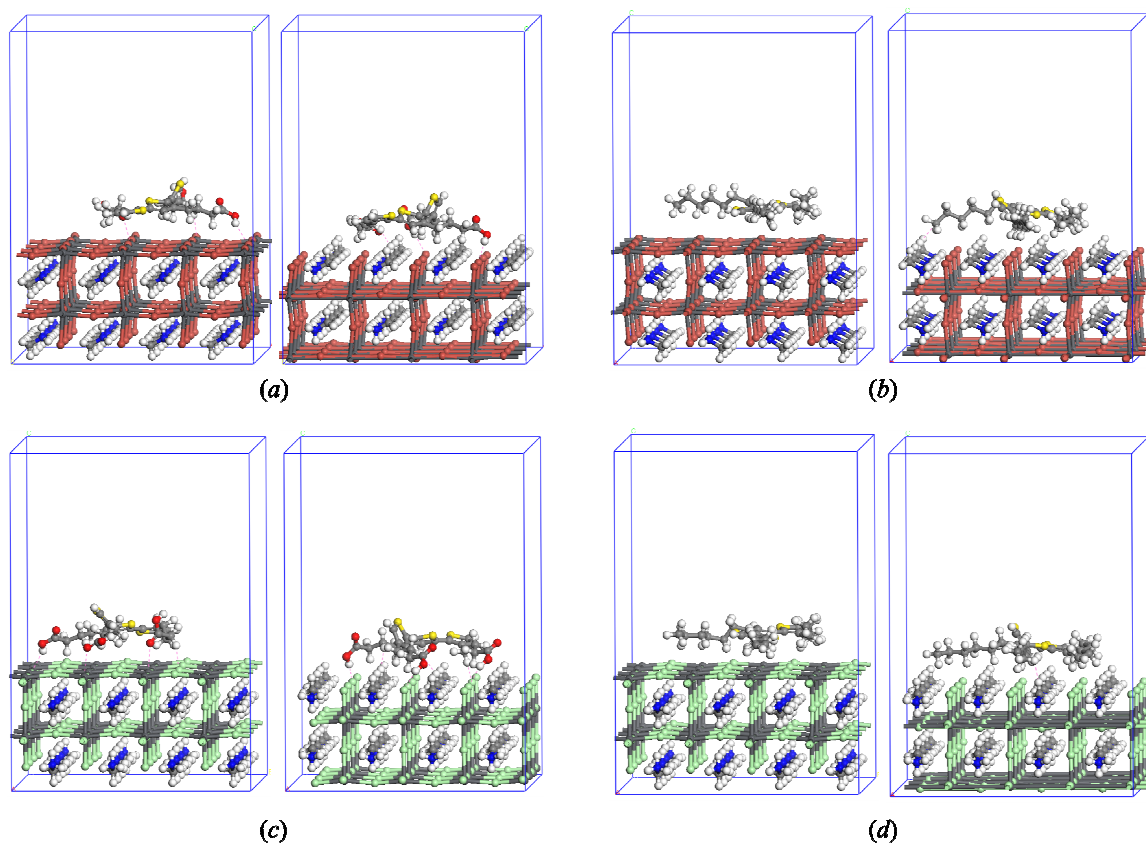
Figure 5, *P3BT* (*a* and *c*) and *P3HT* (*b* and *d*) polymers adsorbed on perovskite surface (*a* and *b* - $CH_3NH_3PbBr_3$; *c* and *d* - $CH_3NH_3PbCl_3$)

Figure 6, MO level (HOMO and LUMO) diagrams on perovskite (left, *a* and *b* - $CH_3NH_3PbBr_3$, *c* and *d* - $CH_3NH_3PbCl_3$) and polymer (right, a and c - *P3BT*, b and d - *P3HT*)**;** (I) on large distance, (II) and (III) adsorbed on surface (correspond to orientations presented on Fig. 5)